Inorganic Chemistry

Article

pubs.acs.org/IC

Anionic Tantalum Dihydride Complexes: Heterobimetallic Coupling Reactions and Reactivity toward Small-Molecule Activation

Thomas G. Ostapowicz and Michael D. Fryzuk*

Department of Chemistry, The University of British Columbia, 2036 Main Mall, Vancouver, British Columbia, Canada

Supporting Information

ABSTRACT: The anionic dihydride complex $[Cp_2TaH_2]^-$ was synthesized as a well-defined molecular species by deprotonation of Cp_2TaH_3 while different solubilizing agents, such as [2.2.2]cryptand and 18-crown-6, were applied to encapsulate the alkali-metal counterion. The ion pairs were characterized by multiple spectroscopic methods as well as X-ray crystallography, revealing varying degrees of interaction between the hydride ligands of the anion and the respective countercation in solution and in the solid state. The $[Cp_2TaH_2]^-$ complex anion shows slow exchange of the hydride ligands when kept under a D_2 atmosphere, but a very fast reaction is observed when $[Cp_2TaH_2]^-$ is reacted with CO_2, from which $Cp_2TaH(CO)$ is obtained as the tantalum-containing reaction product, along with inorganic salts. Furthermore, $[Cp_2TaH_2]^-$ can act as a synthon in heterobimetallic coupling reactions with transition-metal halide complexes. Thus, the heterobimetallic complexes $Cp_2Ta(\mu\text{-}H)_2Rh(dippp)$ and $Cp_2Ta(\mu\text{-}H)_2Ru(H)(CO)(P^iPr_3)_2$ were synthesized and characterized by various spectroscopies and via single-crystal X-ray diffraction. The new hydride bridged tantalum−rhodium heterobimetallic complex is cleaved under a CO atmosphere to yield mononuclear species and slowly exchanges protons and hydride ligands when exposed to D_2 gas.

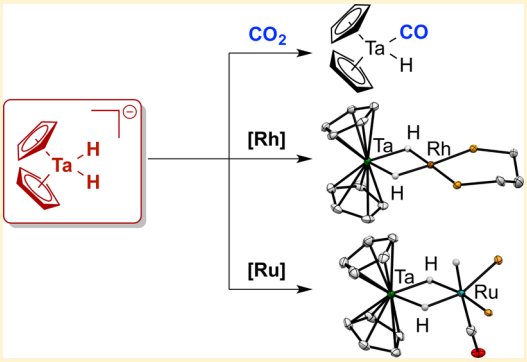

INTRODUCTION

Heterobimetallic complexes have gained much attention because they can potentially allow for a bifunctional activation of small molecules through the cooperation of two electronically distinct metal centers.[1] In particular, if the pair of metals is a combination of an early metal (groups 3−6) and a late metal (groups 7−9), so-called early−late heterobimetallic (ELHB) complexes, there can be applications in homogeneous catalysis.[2] A wide variety of heterobimetallic complexes with bridging hydride ligands have been investigated, several of which are thought to act as intermediates or resting states in catalytic hydrogenation reactions.[3] Therefore, much effort has been dedicated to devising broadly applicable routes to selectively synthesize heterobimetallic complexes possessing bridging hydride ligands and to avoid the formation of homobimetallic species or species with other bridging ligands.[3b,4]

Three main strategies have been developed to provide the selective formation of hydride-bridged heterobimetallic complexes: (i) adduct formation between a nucleophilic hydride complex and an electrophilic metal fragment after ligand displacement;[5] (ii) coupling of a neutral oligohydride complex with a metal alkyl species via protonolysis;[6] (iii) a salt metathesis reaction between an anionic oligohydride complex and a metal halide species. This third method, originally developed by Caulton et al. in 1984,[7] has recently gained much attention, and several heterobimetallic hydride complexes with interesting characteristics and unprecedented reactivity patterns have been synthesized by the groups of Caulton[8] and more recently by Mathieu,[9] Suzuki,[10] and others[11] following the same synthetic approach (Figure 1). Caulton's method is attractive because it is selective and broadly applicable in the synthesis of diverse complexes because of the wide variety of anionic oligohydrides and readily available metal halide complexes.

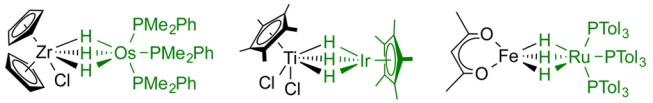

Figure 1. Selected examples of heterobimetallic hydride complexes prepared by the Caulton method via salt metathesis with anionic late-transition-metal oligohydrides (respective anionic oligohydride fragments highlighted in green).

For late transition metals, numerous examples of anionic oligohydride species exist in the literature because they play a crucial role in olefin hydrogenation.[12] Generally, late-transition-metal oligohydrides are accessed either from the deprotonation of neutral hydride complexes[13,8a] or by halide−hydride exchange in the presence of an excess of a hydride reagent,[14] but other methods were developed as well.[15,16] For early transition metals, however, only a few examples of monomeric, anionic oligohydride complexes are described in the literature.[17]

Received: December 12, 2014
Published: February 11, 2015

DOI: 10.1021/ic502976r
Inorg. Chem. 2015, 54, 2357−2366

So far, very limited examples have been described in which an anionic oligohydride complex of an early transition metal was used for the synthesis of heterobimetallic hydride complexes[17b,18] and, to the best of our knowledge, no anionic tantalum hydride complex.

Herein we report the preparation, characterization, and reactivity of well-defined anionic tantalum hydride complexes. One of our long-standing goals is to discover multimetallic hydride complexes that can activate and functionalize small molecules, in particular molecular nitrogen. One intriguing strategy is to devise an ELHB oligohydride system that can accomplish this because we have already discovered the early-transition-metal homobimetallic hydride system $[PhP(CH_2SiMe_2NPh)_2Ta]_2(\mu\text{-}H)_4$, which can activate a number of small molecules such as N_2, CO, CO_2, alkynes, and alkenes.[19] In an effort to investigate the synthesis of potential ELHB oligohydride complexes, we reasoned that a general process in which the late-transition-metal fragment is easily varied while the early-transition-metal fragment remains constant was worth investigating as a way to examine the effect of the late transition metal on small-molecule activation.

RESULTS AND DISCUSSION

Synthesis and Characterization. As a starting point, we targeted anionic tantalum hydride complexes for heterobimetallic coupling reactions. An early report[20] from Green's group mentioned that the treatment of Cp_2TaH_3 with *n*-butyllithium results in the formation of a golden-yellow solid, for which they suggested the composition $\{Cp_2TaH_2Li\}_x$. Later, Smith et al. used this compound in situ as a nucleophile, thus supporting the initial formulation of Green et al.[21] However, neither group reported any NMR data or provided any structural characterization of this compound. In fact, while many examples of cationic species of the general formula $[Cp_2TaH_2(L)]^+$ can be found in the literature,[22] other than the aforementioned reports, there has been no systematic study of the parent anionic tantalocene dihydride of the formula $[Cp_2TaH_2]^-$ to our knowledge. Intrigued by the initial reports of Green et al., we initiated a study to generate $[Cp_2TaH_2]^-$ reproducibly and in high yield and to investigate its reactivity.

The reaction of Cp_3TaH_3 in tetrahydrofuran (THF) with excess KH in the presence of [2.2.2]cryptand proceeds at room temperature over the course of several hours to give upon filtration and crystallization at −35 °C bright-red crystals of **1** in 91% yield (Scheme 1). Compound **1** is almost insoluble in nonpolar solvents such as hexanes, benzene, or toluene but yields a dark-red solution in THF. The ^{1}H NMR spectrum of **1** taken in THF-d_8 reveals a singlet at −10.19 ppm corresponding to a single hydride resonance significantly shifted upfield compared to the hydride signals of the parent Cp_2TaH_3 at −1.63 and −3.01 ppm. The signal of the cyclopentadienyl ligand of **1** at 3.76 ppm is also upfield-shifted compared to the signal of Cp_2TaH_3 at 4.77 ppm. On the basis of the ^{1}H and ^{13}C NMR data, compound **1** was formulated as the salt $[K([2.2.2]\text{-cryptand})][Cp_2TaH_2]$. X-ray crystallography confirmed this formulation, with the $[Cp_2TaH_2]^-$ and $[K([2.2.2]\text{cryptand})]^+$ fragments exhibiting typical bond lengths and angles (Figure 2). The structure of **1** is consistent with an anion−cation pair in the solid state, in which the anion and cation represent well-separated entities. The Ta···K distance of 6.367 Å clearly indicates that there is no interaction of the two complex ions. The two hydride ligands bound to the tantalum center were located independently from the electron density map, freely refined without any restraints, and agree with the observed single ^{1}H NMR hydride signal.

Scheme 1

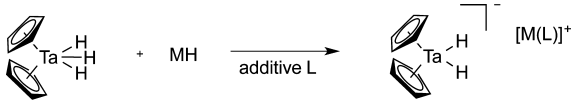

M	additive L	complex
K	[2.2.2]cryptand	**1**
	18-crown-6	**2**
Na	[2.2.2]cryptand	**4**

The reaction of Cp_2TaH_3 with cation-stabilizing agents other than cryptands or different alkali-metal bases yields similar compounds, but the formation of these products is much slower than the deprotonation with the combination of KH and [2.2.2]cryptand. For example, the reaction of Cp_2TaH_3 in THF with excess KH in the presence of 18-crown-6 instead of [2.2.2]cryptand proceeds at room temperature over the course of 5 days; after workup, compound **2** is isolated in 98% yield (Scheme 1). The crown ether derivative **2** is far less soluble even in THF compared to its cryptand counterpart **1**. The ^{1}H NMR spectrum of **2** taken in THF-d_8 is qualitatively very similar to the spectrum of **1**, but the hydride signal is shifted further upfield to −11.22 ppm. ^{1}H and ^{13}C NMR data of **2** are in good agreement with a structure of $[K(18\text{-crown-6})][Cp_2TaH_2]$. The molecular structure of **2** was confirmed (Figure 3) by X-ray analysis using crystals grown from a concentrated THF solution at −35 °C. In stark contrast to the structure of the cryptand derivative **1**, a direct interaction between the anionic tantalum dihydride and potassium cation is observed for **2** in the solid state. The independently located and freely refined hydrides act as bridging ligands between tantalum and potassium, and the Ta···K distance is only 3.771 Å.

If no [2.2.2]cryptand or 18-crown-6 is added during deprotonation of Cp_2TaH_3 with KH at ambient temperatures, deprotonation is not observed even after 2 weeks. This is especially surprising because the related niobium compound, Cp_2NbH_3, is quantitatively deprotonated under similar conditions within 3 days.[18c] Heating a mixture of Cp_2TaH_3 and KH does result in deprotonation, but also partial decomposition is observed; for example, if a mixture of Cp_2TaH_3 and KH is stirred for 2 days at 80 °C in dimethoxyethane (DME), one can isolate bright-red crystals by cooling the solution to −35 °C, which could be identified as $K[Cp_2TaH_2]\cdot KCp$ (**3**) by X-ray crystallography. The equivalent of KCp has presumably formed by decomposition of Cp_2TaH_3 during the course of the reaction. Similar MCp (M = Li, Na, K) elimination from late-transition-metal metallocenes has been reported previously upon treatment with the elemental alkali metals.[23] In the solid-state structure, the two components of **3** are arranged in a three-dimensional framework, in which potassium ions act as nodal points that bridge between two different $[Cp_2TaH_2]^-$ units and a KCp unit (see Figures S4.5 and S4.6 in the Supporting Information, SI). The hydride ligands of $[Cp_2TaH_2]^-$ interact with two KCp units in the framework, resulting in short Ta···K distances of 3.705 and 3.724 Å, respectively. Compound **3** shows very low solubility in toluene, diethyl ether, or hexanes and also poor solubility in THF. In the ^{1}H NMR spectrum of **3** in THF-d_8, one signal for

DOI: 10.1021/ic502976r
Inorg. Chem. 2015, 54, 2357−2366

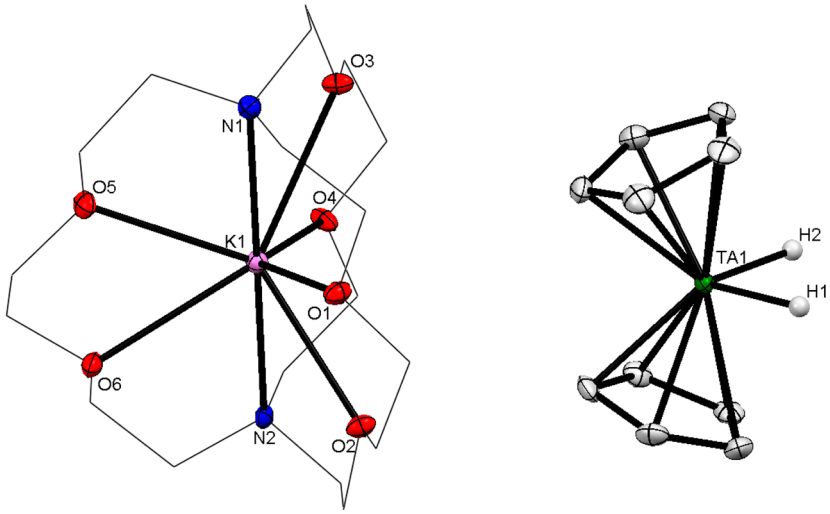

Figure 2. ORTEP representation of the solid-state molecular structure of **1** with ellipsoids drawn at 50% probability. Hydrogen atoms, except H1 and H2, were omitted for clarity. Parts of the cryptand framework are shown as a wireframe representation for clarity. Selected distances and bond lengths (Å) and angles (deg): Ta1···K1, 6.367; Ta1−H1, 1.71(3); Ta1−H2, 1.72(3); Ta1−$Cp1_{plane}$, 2.009; Ta1−$Cp2_{plane}$, 2.012; K1−N1, 3.056(2); K1−O1, 2.811(2); H1−Ta1−H2, 81.78; $Cp1_{centroid}$−Ta1−$Cp2_{centroid}$, 129.46; N1−K1−N2, 179.57(6).

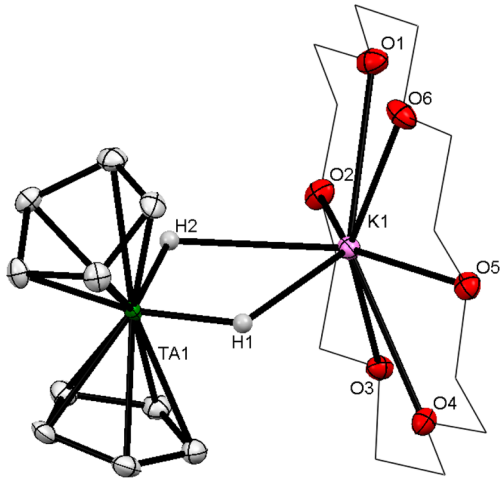

Figure 3. ORTEP representation of the solid-state molecular structure of **2** with ellipsoids drawn at 50% probability. Hydrogen atoms, except H1 and H2, were omitted for clarity. Parts of the crown ether framework are shown as a wireframe representation for clarity. Selected distances and bond lengths (Å) and bond angles (deg): Ta1···K1, 3.7708(12); Ta1−H1, 1.73(4); Ta1−H2, 1.78(4); K1−H1, 2.91(4); K1−H2, 2.71(4); Ta1−$Cp1_{plane}$, 2.014; Ta1−$Cp2_{plane}$, 2.017; K1−O1, 2.968(2); H1−Ta−H2, 88.5(19); $Cp1_{centroid}$−Ta1−$Cp2_{centroid}$, 145.89; O1−K1−O4, 147.92(6).

the Cp protons of $[Cp_2TaH_2]^-$ at 3.95 ppm and a small signal for KCp[24] at 5.76 ppm could be observed. However, the signal for the hydride ligands is −11.42 ppm, even further shifted to the upfield region than the crown ether derivative **2**.

When NaH is used as the base instead of KH in combination with [2.2.2]cryptand, the deprotonation requires 2 weeks at ambient temperature until all of the Cp_2TaH_3 starting material is consumed. After workup, compound **4** is obtained as an orange-brown crystalline solid (Scheme 1). If the reaction mixture is heated in order to accelerate deprotonation, partial decomposition of the tantalum starting material is observed to form [Na([2.2.2]cryptand)]Cp, which shows a Cp resonance at 5.47 ppm by ^{1}H NMR and at 103.4 ppm by ^{13}C NMR. The desired product **4**, however, reveals a hydride signal as a broad singlet at −10.73 ppm, and the Cp protons resonate at 3.83 ppm in the ^{1}H NMR spectrum. The solid-state molecular structure of **4** is very similar to the potassium analogue **1**. The $[Cp_2TaH_2]^-$ and the [Na([2.2.2]cryptand)]$^+$ ions are distinct fragment ions without any direct molecular interaction (Figure 4). Both hydride ligands could be located on the Fourier density map and refined without any constraints. Because of its smaller ionic radius, the sodium ion is not symmetrically bound to the cryptand compared with the potassium ion in **1**. The Na1−N1 distance is, at 2.693 Å, significantly shorter than the Na1−N2 distance of 3.282 Å.

A comparison of the ^{1}H NMR spectra of the anionic tantalum dihydrides $[Cp_2TaH_2]^-$ **1**−**4** with different cations reveals a trend of the chemical shift for the hydride ligand. For the [2.2.2]cryptand derivatives **1** and **4**, the signals of the hydride ligands are observed at −10.19 and −10.73 ppm, respectively, whereas the hydride signals in the 18-crown-6 derivative **2** appears at −11.22 ppm and also at −11.42 ppm for the adduct **3**, which does not possess a sequestered K^+ or Na^+ counterion. On the basis of the solid-state structures of the complexes, this trend agrees well with the degree of interaction between the hydride ligands and the alkali-metal counterion. ^{1}H NMR NOESY experiments were conducted in order to probe the aggregation behavior in solution and to determine whether contact or solvent-separated ion pairs are predominantly present in solution for complexes **1** and **2** (see the SI for the spectra). No magnetic exchange between the nuclei over space could be observed for the protons of the cyclopentadienyl ring and cryptand in complex **1**. For complex **2**, however, the nuclear-spin polarization of the cyclopentadienyl protons and the protons of the crown ether was evident. These findings indicate that **1** can be considered as a solvent-separated ion pair in solution, at least on the time scale of NMR experiments. The 18-crown-6 complex **2**, however, exists as a contact ion pair in solution, which could be also described as a heterobimetallic tantalum−potassium complex with two hydride ligands bridging the two metal centers.

An interesting feature of the formation of $[Cp_2TaH_2]^-$ is the color change from the colorless starting material Cp_2TaH_3 to an intense-red product. Upon deprotonation of Cp_2TaH_3 to

DOI: 10.1021/ic502976r
Inorg. Chem. 2015, 54, 2357−2366

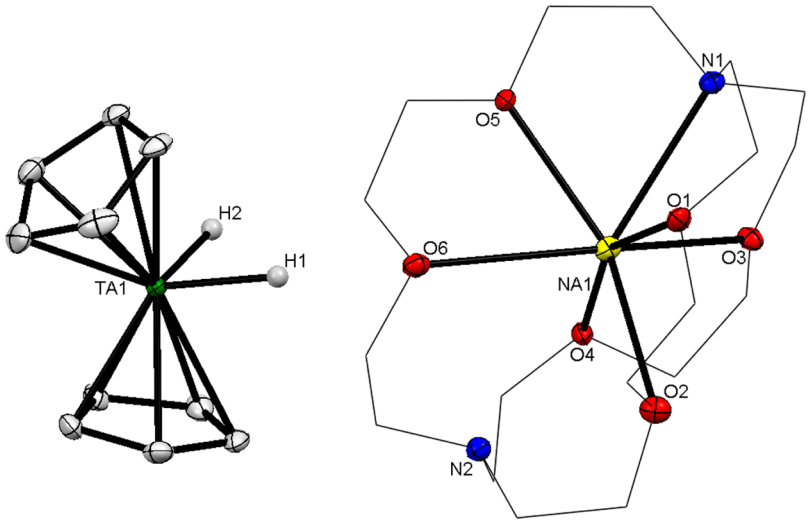

Figure 4. ORTEP representation of the solid-state molecular structure of **4** with ellipsoids drawn at 50% probability. Hydrogen atoms, except H1 and H2, were omitted for clarity. Parts of the cryptand framework are shown as a wireframe representation for clarity. Selected distances and bond lengths (Å) and bond angles (deg): Ta1···Na1, 7.015; Ta1−H1, 1.71(2); Ta1−H2, 1.80(3); Ta1−$Cp1_{plane}$, 2.007; Ta1−$Cp2_{plane}$, 2.011; Na1−N1, 2.693(2); Na1−O1, 2.4926(17); H1−Ta−H2, 80.97; $Cp1_{centroid}$−Ta1−$Cp2_{centroid}$, 146.65.

form $[Cp_2TaH_2]^-$, a change of the formal oxidation state from Ta^V to Ta^{III} occurs. The product is thus isoelectronic to the bright-yellow tungsten complex Cp_2WH_2.[25] In order to investigate the electronic structure of the complexes in more detail, UV−vis spectra were taken of the starting material and the anionic complexes (Figure 5). Cp_2TaH_3 does not show any

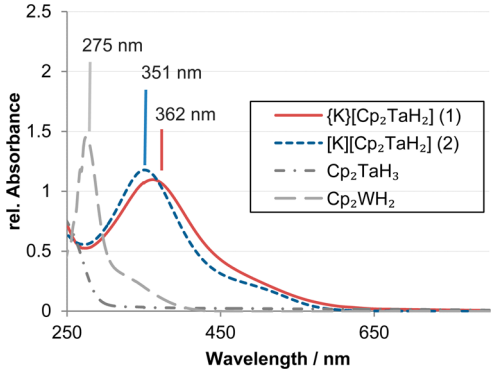

Figure 5. UV−vis absorption spectra of complexes **1**, **2**, Cp_2TaH_3, and Cp_2WH_2 in THF taken at ambient temperature [c = 0.151 (**1**), 0.289 (**2**), and 0.151 (Cp_2WH_2) μmol mL^{-1}].

bands in the visible region, and only a small shoulder feature can be found at 270 nm. In contrast, the anionic dihydride complexes show a distinct band with λ_{max} at 362 nm (ε_{362} = 6400 L mol^{-1} cm^{-1}) for complex **1** and at 351 nm (ε_{351} = 4010 L mol^{-1} cm^{-1}) for complex **2**, both having a broad shoulder at about 500 nm. For comparison, the spectrum of the isoelectronic compound Cp_2WH_2 shows similar features, but the signals are shifted toward shorter wavelengths, exhibiting λ_{max} at 275 nm (ε_{275} = 5200 L mol^{-1} cm^{-1}) and a broad shoulder at about 350 nm. As deduced from the absorption coefficients, metal−ligand charge-transfer transitions are most likely responsible for the major absorptions, and the corresponding energy gap is shifted to higher energy for Cp_2WH_2 compared to $[Cp_2TaH_2]^-$.

Reactivity Studies. The reactivity of the anionic tantalum dihydride complex $[Cp_2TaH_2]^-$ toward small molecules was investigated using the cryptand derivative **1** because this complex has the highest solubility in organic solvents. For the parent compound Cp_2TaH_3, hydrogen−deuterium (H−D) exchange of the hydride ligands occurs under a D_2 atmosphere or in deuterated benzene when thermally or photochemically initiated[26] and is proposed to proceed via the transient Ta^{III} species Cp_2TaH, which then undergoes oxidative addition of D_2. This Cp_2TaH intermediate can also be trapped as $Cp_2Ta(H)(L)$, with L being CO or phosphine ligands.[26a,27] Compound **1** also undergoes H−D exchange when placed under D_2 gas in nondeuterated THF. In this experiment after 9 days, a new signal in the ^2H NMR spectrum could be observed at −10.3 ppm, which can be assigned to $[Cp_2TaD_2]^-$ or $[Cp_2TaHD]^-$. In the ^1H NMR spectrum of the same sample, however, the parent signal at −10.4 ppm is still present. Therefore, H−D exchange of the hydride ligands in $[Cp_2TaH_2]^-$ with D_2 does occur, even at ambient temperature and without thermal or intensive photochemical initiation, but the rate of the observed exchange is very slow.

Complex **1** reacts readily at low temperature with CO_2. If a THF solution of **1** is frozen and CO_2 is introduced, a bright-purple solution forms upon thawing along with precipitation of a colorless solid. After filtration and removal of the solvent, a purple powder was obtained (Scheme 2). The ^1H NMR

Scheme 2

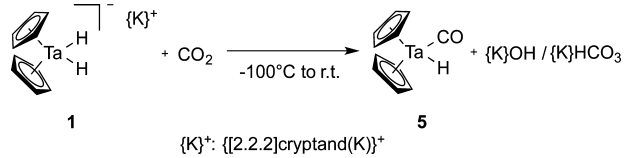

spectrum of this newly formed species reveals a single hydride resonance at −6.77 ppm and a signal corresponding to two cyclopentadienyl rings at 4.48 ppm as a doublet with a very small coupling constant of 0.5 Hz. In the ^{13}C NMR spectrum, the signal for the Cp rings is observed at 82.7 ppm. The purple reaction product was identified as $Cp_2TaH(CO)$ (**5**) based on a comparison with literature values.[26b,28] The reaction of

DOI: 10.1021/ic502976r
Inorg. Chem. 2015, 54, 2357−2366

$[Cp_2TaH_2]^-$ with CO_2 provides therefore an alternative synthesis for **5**, which is usually prepared using CO gas and high temperatures.[26b,27] The colorless byproduct of the reaction shows a very low solubility in hexanes, toluene, or THF but a moderate solubility in pyridine, dimethyl sulfoxide (DMSO), or water. The ^{1}H NMR spectrum in DMSO-d_6 contains three major signals of cryptand and a very small resonance at 8.58 ppm. In the ^{13}C NMR spectrum, however, three signals in the low-field region at 164.7, 168.7, and 173.3 ppm can be observed next to the cryptand signals at 53.2, 67.0, and 69.8 ppm. The three low-field signals can be assigned to HCO_3^-, CO_3^{2-}, and HCO_2^-, respectively, by a comparison with literature values.[29] The signal in the ^{1}H NMR spectrum at 8.58 ppm can be assigned to the formate anion HCO_2^-; from integration of the ^{1}H NMR signals, it can be deduced that the fraction of formate in the overall composition is quite small, estimated to be less than 5%. On the basis of the NMR evidence, the white solid obtained as the byproduct of the formation of **5** is therefore a mixture of the $[K([2.2.2]cryptand)]^+$ cation with bicarbonate and carbonate counterions as major components as well as with formate as a minor component. Furthermore, the presence of $[K([2.2.2]cryptand)]OH$ is very likely but could not be directly observed by NMR techniques. It is not obvious how this process occurs. There are examples of tantalum hydride complexes that add to CO_2 to generate formate species initially,[30] but the formation of CO is counterintuitive for an early transition metal like tantalum. Nevertheless, we present this transformation here to help describe the overall reactivity patterns of this dihydride anion.

With respect to our principle goal of preparing ELHB complexes, we investigated the reaction with certain rhodium and ruthenium precursors. Upon the addition of a solution of $[RhCl(dippp)]_2$ [dippp = 1,3-bis(diisopropylphosphino)-propane] at ambient temperature to a dark-red solution of **1** in THF, an immediate color change to brown is observed (Scheme 3). After workup, the heterobimetallic compound

Scheme 3

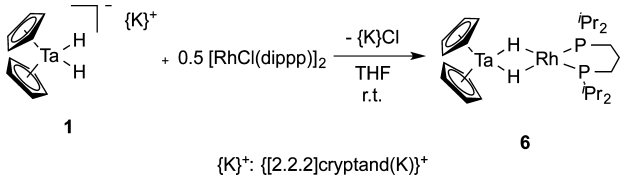

$Cp_2Ta(\mu\text{-}H)_2Rh(dippp)$ (**6**) can be isolated as a microcrystalline intensely red powder. The heterobimetallic compound is highly soluble in various solvents such as toluene, benzene, diethyl ether, and THF and even in very nonpolar solvents such as hexanes or pentane.

In the ^{31}P NMR spectrum of **6** taken in C_6D_6, a doublet resonance is observed at 39.8 ppm ($^1J_{RhP}$ = 143 Hz), and the ^{1}H NMR spectrum of **6** reveals a new hydride signal at −15.26 ppm that exhibits a higher order splitting pattern due to scalar coupling to ^{103}Rh and the two ^{31}P nuclei (Figure 6); for the related heterobimetallic complex $Cp_2Ta(\mu\text{-}H)(\mu\text{-}Cl)Rh(dppe)$ [dppe = 1,2-bis(diphenylphosphino)ethane], phosphorus resonances were reported at 79.0 and 43.0 ppm, and the bridging hydride signal was found at −12.61 ppm, indicating a more electron-deficient electronic environment[5b] than that in **6**.[5] Only one signal for both cyclopentadienyl rings can be found in the ^{1}H NMR spectrum of **6**, and two signals are present for the

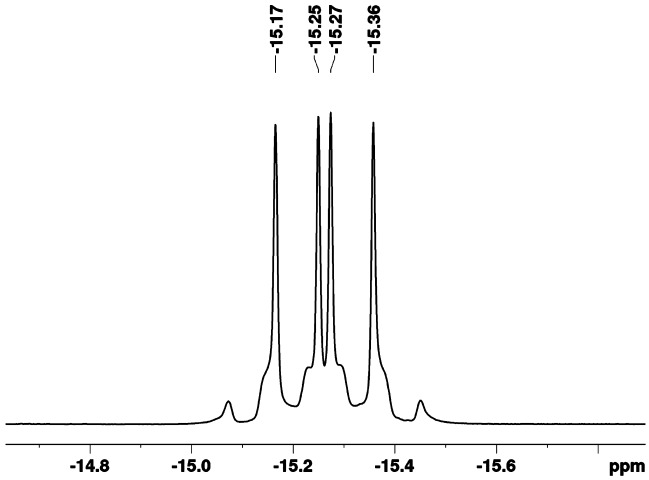

Figure 6. ^{1}H NMR spectrum of the hydride signal of complex **6**, measured in C_6D_6 at 400 MHz.

isopropyl groups in the ^{1}H and ^{13}C NMR spectra of **6**, as expected.

To compare the electronic structure of **6** to the anionic species $[Cp_2TaH_2]^-$, UV−vis absorption spectra were recorded. An orange-red solution of **6** in THF shows a remarkably different electronic spectrum compared to those obtained for **1** and **2** (cf. Figure 5). Three relatively sharp bands are observed in the UV region with λ_{max} at 227, 305, and 368 nm as well as one broad band at about 500 nm (Figure 7).

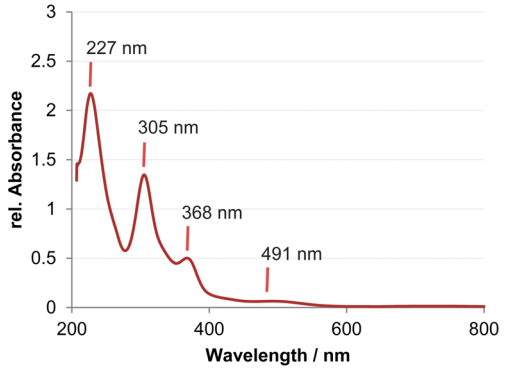

Figure 7. UV−vis absorption spectrum of complex **6** in THF taken at ambient temperature (c = 0.091 μmol mL^{-1}).

Furthermore, the molar absorptivity ε_{305} = 15900 L mol^{-1} cm^{-1} is about 3 times as high as that observed for the monomeric $[Cp_2TaH_2]^-$ derivative **1** or **2**. The distinct electronic transitions, together with the intense absorbance of the heterobimetallic compound **6**, could result from charge-transfer processes or from direct metal-to-metal interactions.[31]

Crystals suitable for X-ray diffraction could be obtained by cooling a concentrated solution of **6** to −35 °C for several days. The compound crystallizes in the space group $P2_1/c$ in a monoclinic system. The independent molecular unit shows the rhodium center in a square-planar coordination environment. The two bridging hydride ligands were located from the electron density map and optimized without restrictions. An interesting feature of the molecular structure of **6** is the very short Ta1−Rh1 distance of only 2.7236(8) Å. This is much smaller than the sum of the covalent radii of rhodium (1.42 Å)[32] and tantalum (1.70 Å),[32] which could be further evidence

DOI: 10.1021/ic502976r
Inorg. Chem. 2015, 54, 2357−2366

of some kind of interaction between tantalum and rhodium in compound **6** (Figure 8).

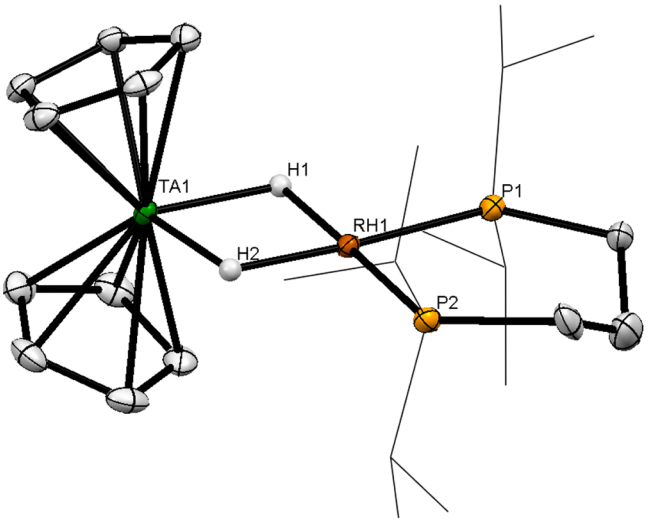

Figure 8. ORTEP representation of the solid-state molecular structure of **6** with ellipsoids drawn at 50% probability. All hydrogen atoms, except H1 and H2, were omitted for clarity. Isopropyl groups are shown as wireframe representations for clarity. Selected distances and bond lengths (Å) and bond angles (deg): Ta1···Rh1, 2.7236(8); Ta1−H1, 1.91(3); Ta1−H2, 1.91(3); Rh1−H1, 1.76(3); Rh1−H2, 1.72(3); Ta1−$Cp1_{plane}$, 2.027; Ta1−$Cp2_{plane}$, 2.029; Rh1−P1, 2.2221(9); Rh1−P2, 2.2166(8); H1−Ta1−H2, 78.62; H1−Rh1−H2, 88.06; $Cp1_{centroid}$−Ta1−$Cp2_{centroid}$, 142.96; P1−Rh1−P2, 95.03(4); Ta1−Rh1−P1, 132.12(3); Ta1−Rh1−P1, 132.85(2).

The reactivity of **6** with small molecules such as H_2 and CO was investigated. Exposure of a C_6D_6 solution of **6** to 4 atm of H_2 in a flame-sealed NMR tube did not show any change as monitored by ^1H or ^{31}P NMR spectroscopy compared to pure **6**. When **6** is exposed to D_2, however, after 24 h a new signal appears in the ^2H NMR spectrum of the reaction mixture at −15.3 ppm that can be assigned to the bridging Ta(μ-D)$_2$Rh deuteride ligands (see the SI for spectra). Furthermore, deuterium is also incorporated into the cyclopentadienyl rings and to a smaller extent even into the methyl groups of the isopropyl moieties at the phosphorus donor atom. Given the very slow reaction of D_2 with the parent $[Cp_2TaH_2]^-$ anion in **1**, it is interesting to note that H−D exchange occurs in **6** quite readily with D_2. Because upon the addition of H_2 to **6** no change can be observed in the ^1H and ^{31}P NMR spectra, it can be concluded that an adduct forms, but the equilibrium lies on the side of the starting heterobimetallic **6** + H_2.

Exposure of **6** to 4 atm of CO gas in C_6D_6 results in the cleavage of the heterobimetallic species and the formation of monomers. The tantalum product is easily identified as **5** because it matches exactly the same spectroscopic data as those seen before from the reaction of **1** with CO_2.[26b] The mixture also displays a new hydride signal, which appears as a triplet of doublets (J = 50.4 and 11.5 Hz) at −9.62 ppm in the ^1H NMR spectrum, one new doublet ($^1J_{RhP}$ = 112.4 Hz) in the $^{31}P\{^1H\}$ NMR spectrum at 39.9 ppm, and one new doublet of triplets at 201.3 ppm (J = 68.7 and 9.1 Hz) in the $^{13}C\{^1H\}$ NMR spectrum assigned for a rhodium-bound CO ligand. On the basis of the spectroscopic data and by a comparison with literature values, the five-coordinate Rh(H)(CO)$_2$(dippp) (**7**) is the second product of the reaction (Scheme 4).[33]

Scheme 4

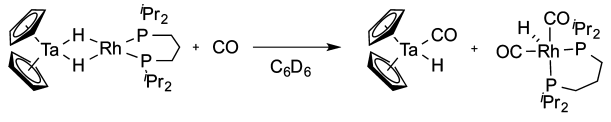

To extend the use of the anion $[Cp_2TaH_2]^-$ in the formation of ELHB complexes, we examined the reaction of **1** with the chloride complexes Ru(H)(Cl)(CO)(P^{i}Pr$_3$)$_2$ and Ru(H)(Cl)-(N$_2$)(P^{i}Pr$_3$)$_2$ (Scheme 5). However, these reactions were more

Scheme 5

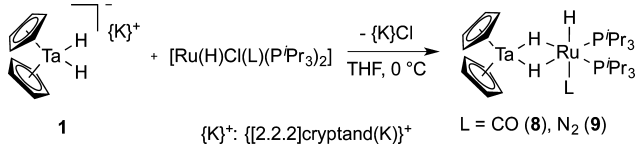

complex, and it was difficult to obtain pure heterobimetallic products. The optimal conditions were found to be cooling a solution of **1** to 0 °C and the slow addition of a ruthenium chloride species to it. Even so, the resulting heterobimetallic species **8** and **9** could only be obtained in approximately 80% purity based on NMR data. The purification of the two heterobimetallic compounds by recrystallization was drastically impeded by the very high solubility of **8** and **9** as well as a very similar solubility of the respective impurities even in pentane at −35 °C.

Despite the presence of impurities, spectroscopic studies show very interesting similarities and differences between the CO and N_2 derivatives **8** and **9** that provide useful structural information for these complexes. Both compounds show very similar chemical shifts in the $^{31}P\{^1H\}$ NMR spectra at 70.0 and 71.3 ppm for **8** and **9**, respectively, which indicates an overall similar structural arrangement of the phosphorus ligands in both complexes. In the ^1H NMR spectra for both complexes, two distinct signals for the cyclopentadienyl ligands can be observed showing different chemical environments. For the CO derivative **8**, the two singlets appear rather close together at 5.67 and 5.64 ppm, whereas in the N_2 derivative, the two signals are quite separated at 5.25 and 4.36 ppm. Also for both complexes, two hydride signals in the ratio of 1:2 can be assigned to two bridging hydrides and one terminal hydride. In both cases, the splitting of the signals can be best described as a triplet of triplets for the signal integrating to one proton and a higher-order multiplet integrating to two protons. In both complexes, the signals for the two bridging hydrides have very similar chemical shifts at −17.99 ppm (**8**) and −16.50 ppm (**9**). The chemical shift of the terminal hydride ligand, however, changes dramatically; for the CO complex **8**, the signal is found at −6.55 ppm, whereas the N_2 species has its signal for the terminal hydride at −24.94 ppm (Figure 9). On the basis of all of the spectroscopic data, the structures of both of these complexes are proposed to be very similar to the ruthenium center in an octahedral environment with the cis phosphine donors in the same plane as the bridging hydride ligands and the terminal hydride ligand either trans to the CO ligand in **8** or trans to the N_2 moiety in **9**. The possibility of N_2 dissociation during the coupling reaction cannot be completely ruled out; however, the presence of an absorption at 2097 cm^{-1} in the IR

DOI: 10.1021/ic502976r
Inorg. Chem. 2015, 54, 2357−2366

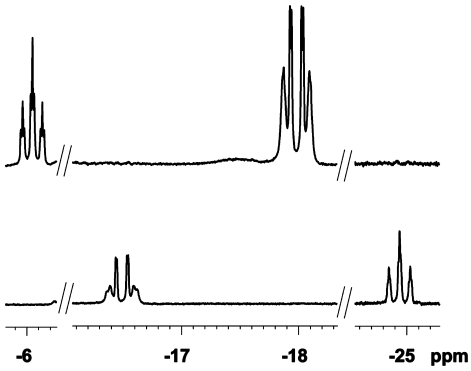

Figure 9. Comparison of the ^{1}H NMR hydride signals for complexes **8** (top) and **9** (bottom) measured in C_6D_6 at 400 MHz.

spectrum of compound **9** serves as further support for the proposed structure of complex **9** (see the SI).

For the CO derivative **8**, single crystals were obtained from concentrated pentane solutions at −35 °C over several weeks. The compound crystallizes in the space group $P2_1/n$ in the monoclinic system. The molecular unit reveals the ruthenium center in a distorted octahedral coordination environment (Figure 10). As suggested based on the NMR spectroscopic

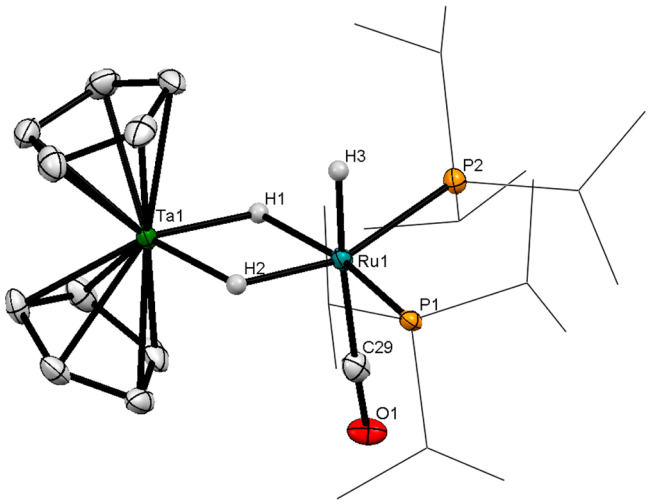

Figure 10. ORTEP representation of the solid-state molecular structure of **8** with ellipsoids drawn at 50% probability. Hydrogen atoms, except H1, H2, and H3, were omitted for clarity. Isopropyl groups are shown as wireframe representations for clarity. Selected distances and bond lengths (Å) and bond angles (deg): Ta1···Ru1, 2.8677(7); Ta1−$Cp1_{plane}$, 2.042; Ta1−$Cp2_{plane}$, 2.046; Ru1−P1, 2.366(2); Ru1−P2, 2.349(1); Ru1−C29, 1.899(6); C29−O1, 1.155(7); $Cp1_{centroid}$−Ta1−$Cp2_{centroid}$, 135.81; P1−Ru1−P2, 108.93(5); Ta1−Ru1−P1, 123.56(4); Ta1−Ru1−P2, 124.96(4); Ru1−C29−O1, 177.9(5).

data, the two phosphorus ligands are in-plane with the bridging hydride ligands, leaving the two apical positions for CO and the third hydride ligand. For this complex, the hydride ligands had to be geometrically constrained to allow for refinement of the structure. Reminiscent of the rhodium complex **6**, the bond distance between tantalum and ruthenium in **8** is rather short at only 2.8677(7) Å. Also, in this case, this distance is shorter than the sum of the covalent radii of tantalum (1.70 Å)[32] and ruthenium (1.46 Å),[32] suggesting an interaction between the two metal centers as in the case of compound **6**.

CONCLUSIONS

The results of this study demonstrate that Cp_2TaH_3 can be cleanly deprotonated to give the anionic dihydride complex $[Cp_2TaH_2]^-$ as a well-defined molecular species. When the potassium or sodium cation is ligated by [2.2.2]cryptand, the two ions are completely separated, whereas the use of 18-crown-6 with the potassium cation results in an interaction with the hydride ligands, which can be observed in the solid state as well as in solution. Because of the higher solubility in organic solvents, the [2.2.2]cryptand derivative **1** was found to be a convenient starting material to explore the further reactivity of the $[Cp_2TaH_2]^-$ anion. When $[Cp_2TaH_2]^-$ is treated with gaseous CO_2, **5** is formed as the only tantalum-containing reaction product, while a hydride ligand of $[Cp_2TaH_2]^-$ is transferred to CO_2. The treatment of $[Cp_2TaH_2]^-$ with the appropriate rhodium or ruthenium halide complexes leads to the formation of **6** and $Cp_2Ta(\mu\text{-}H)_2Ru(H)(L)(P^iPr_3)_2$ (L = CO, N_2), respectively. Thus, this method allows for the synthesis of ELHB oligohydride complexes in which the late-transition-metal fragment can be varied while the early-transition-metal fragment remains constant, complementing the currently used procedures for the synthesis of such types of complexes. The spectroscopic and crystallographic features of the reported heterobimetallic complexes suggest a very close proximity of the two metal centers below the sum of their van der Waals radii. When exposed to small molecules such as CO or H_2, the heterobimetallic tantalum−rhodium compound is cleaved to yield mononuclear species that are stable in the case of CO and transient in the case of H_2. The heterobimetallic species could therefore serve as resting states in catalytic cycles, while the active mononuclear species are only formed when substrates are available. The further exploration of their reactivity toward small-molecule activation and catalytic applications is an ongoing interest in our research group.

EXPERIMENTAL SECTION

General Considerations. All air- and moisture-sensitive manipulations were carried out using standard vacuum-line, Schlenk, and cannula techniques or in an Innovative Technologies inert-atmosphere drybox under an atmosphere of purified oxygen-free N_2. THF, toluene, and diethyl ether were dried using a solvent purification system from Innovative Technologies, by passage through towers containing activated alumina and molecular sieves. DME and pentane were distilled from sodium/benzophenone, degassed through freeze−pump−thaw cycles, and stored over molecular sieves. Benzene-d_6 was purchased from Cambridge Isotope Laboratories, refluxed over sodium benzophenone, vacuum-transferred, and degassed through freeze−pump−thaw cycles. THF-d_8 was purchased from Cambridge Isotope Laboratories, dried over activated 4 Å molecular sieves, and freeze−pump−thaw degassed. Cp_2WH_2 was purchased from Alfa Aesar and used as received. The following compounds were prepared according to literature procedures: Cp_2TaH_3,[34] $[RhCl(dippp)]_2$,[35] $Ru(H)(Cl)(CO)(P^iPr_3)_2$,[36] $Ru(H)(Cl)(N_2)(P^iPr_3)_2$.[37]

^{1}H, ^{31}P, and ^{13}C NMR spectra were recorded on a Bruker AV-300 MHz or AV-400 MHz spectrometer. Unless noted otherwise, all spectra were recorded at ambient temperature. ^{1}H NMR spectra were referenced to a residual proton signal in C_6D_6 (7.16 ppm), DMSO-d_6 (2.50 ppm), pyridine-d_5 (7.19 ppm), or THF-d_8 (1.72 ppm); ^{31}P NMR spectra were referenced to 85% H_3PO_4 at 0.0 ppm; ^{13}C NMR spectra were referenced to the solvent resonance of C_6D_6 (128.0 ppm), DMSO-d_6 (39.5 ppm), or THF-d_8 (25.31 ppm). Assignments of the signals were made on the basis of COSY, HSQC, and HMBC NMR experiments. UV−vis spectra were recorded on a Varian Cary 5000 UV−vis−near-IR spectrophotometer at ambient temperatures.

DOI: 10.1021/ic502976r
Inorg. Chem. 2015, 54, 2357−2366

Microanalyses (C, H, and N) were performed at the Department of Chemistry at the University of British Columbia.

Synthesis of [K([2.2.2]cryptand)][Cp_2TaH_2] (1). At ambient temperature, a solution of Cp_2TaH_3 (100 mg, 0.32 mmol) in 5 mL of THF was added to a slurry of KH (41 mg, 1.02 mmol) and [2.2.2]cryptand (126 mg, 0.33 mmol) in 5 mL of THF. The reaction mixture was stirred for 18 h, by which time the initially colorless slurry became dark red. Subsequently, the reaction mixture was filtered through diatomaceous earth and placed in the freezer at −35 °C for 2 days. The obtained bright-red crystals were filtered off, washed with cold THF and diethyl ether, and dried in vacuo to yield 210 mg (0.29 mmol, 91%) of analytically pure compound **1**.

^{1}H NMR (THF-d_8, 400 MHz): δ 3.76 (s, 10H, *Cp*), 3.58 (s, 12H, *cryptand*), 3.53 (t, $^3J_{HH}$ = 5 Hz, 12H, *cryptand*), 2.54 (t, $^3J_{HH}$ = 5 Hz, 12H, *cryptand*), −10.19 (s, 2H, Ta*H*). ^{13}C{^{1}H} NMR (THF-d_8, 101 MHz): δ 71.2 (s, *cryptand*), 69.8 (s, *Cp*), 68.6 (s, *cryptand*), 55.1 (s, *cryptand*). UV−vis (298 K, THF): 362 nm (ε_{362} = 6400 L mol^{-1} cm^{-1}). Anal. Calcd for $C_{28}H_{48}KN_2O_6Ta$: C, 46.15; H, 6.64; N, 3.84. Found: C, 45.85; H, 6.58; N, 4.14.

Synthesis of [K(18-crown-6)][Cp_2TaH_2] (2). At ambient temperature, a solution of Cp_2TaH_3 (100 mg, 0.32 mmol) in 6 mL of THF was added to a slurry of KH (40 mg, 1.00 mmol) and 18-crown-6 (85 mg, 0.32 mmol) in 8 mL of THF. The reaction mixture was stirred for 5 days, by which time the initially colorless slurry became red. Subsequently, the reaction mixture was filtered through diatomaceous earth, and the remaining red solid was washed with 50 mL of THF in small portions until the filtrate was almost colorless. The combined THF fractions were evaporated to dryness, and the resulting red solid was washed three times with 5 mL of diethyl ether. After drying in vacuo, compound **2** was obtained as a red powder in 195 mg yield (0.32 mmol, 98%).

^{1}H NMR (THF-d_8, 400 MHz): δ 3.94 (s, 10H, *Cp*), 3.61 (s, 24H, *crown ether*), −11.22 (s, 2H, Ta*H*). ^{13}C{^{1}H} NMR (THF-d_8, 101 MHz): δ 71.0 (s, *crown ether*), 70.9 (s, *Cp*). UV−vis (298 K, THF): 351 nm (ε_{351} = 4010 L mol^{-1} cm^{-1}) nm. Anal. Calcd for $C_{22}H_{36}KO_6Ta$: C, 42.86; H, 5.89. Found: C, 43.05; H, 5.93.

Synthesis of K[Cp_2TaH_2]·KCp (3). At ambient temperature, a solution of Cp_2TaH_3 (50 mg, 0.16 mmol) in 8 mL of DME was added to a slurry of KH (19 mg, 0.47 mmol) in 4 mL of DME in a Schlenk bomb equipped with a Teflon valve. The reaction mixture was stirred for 2 days in an 80 °C oil bath, by which time the initially colorless slurry became dark brown. Subsequently, the reaction mixture was taken to dryness. The crude product was extracted with 2 × 2 mL of THF and filtered through diatomaceous earth, and the filtrate was placed in the freezer at −35 °C overnight. The resulting red crystals were filtered off, washed with THF and diethyl ether, and dried in vacuo to obtain **3** in 15 mg yield (32.8 μmol, 21%).

^{1}H NMR (THF-d_8, 400 MHz): δ 5.76 (s, K*Cp*), 3.95 (s, 10H, *Cp*), −11.42 (s, 2H, Ta*H*). ^{13}C{^{1}H} NMR (THF-d_8, 101 MHz): δ 71.35 (s, *Cp*).

Synthesis of [Na([2.2.2]cryptand)][Cp_2TaH_2] (4). At ambient temperature, a solution of [Cp_2TaH_3] (50 mg, 0.16 mmol) in 6 mL of THF was added to a slurry of NaH (38 mg, 1.58 mmol) and [2.2.2]cryptand (63 mg, 0.17 mmol) in 6 mL of THF. The reaction mixture was stirred for 2 weeks, by which time the initially colorless slurry became red. Subsequently, the reaction mixture was filtered through diatomaceous earth, and the remaining red solid was washed with 10 mL of THF in small portions until the filtrate was almost colorless. The combined THF fractions were evaporated to dryness, and the resulting red solid was washed three times with 5 mL of diethyl ether. After drying in vacuo, compound **4** was obtained as a red powder in 85 mg yield (0.12 mmol, 74%).

^{1}H NMR (THF-d_8, 400 MHz): δ 3.83 (s, 10H, *Cp*), 3.58 (s, 12H, *cryptand*), 3.54 (t, *J* = 5.0 Hz 12H, *cryptand*), 2.60 (t, *J* = 5.0 Hz, 12H, *cryptand*), −10.73 (br s, 2H, Ta*H*). ^{13}C(^{1}H) NMR (THF-d_8, 101 MHz): δ 70.66 (s, *Cp*). ^{13}C{^{1}H} NMR (THF-d_8, 101 MHz): δ 70.5 (s, *Cp*), 70.2 (s, *cryptand*), 69.4 (s, *cryptand*), 54.7 (s, *cryptand*). Anal. Calcd for $C_{28}H_{48}N_2NaO_6Ta$: C, 47.19; H, 6.79; N, 3.93. Found: C, 47.27; H, 6.81; N, 3.88.

Reaction of 1 toward CO_2. ***Caution!*** *This reaction can result in a pressure of 1.5 atm or greater within a sealed vessel upon warming to room temperature and was performed with great care and always manipulated behind a glass shield.* At ambient temperature, complex **1** (190 mg, 0.26 mmol) was dissolved in 15 mL of THF, and the solution was placed in a thick-walled Schlenk tube sealed with a Teflon valve. The solution was degassed three times via freeze−pump−thaw cycles, and the reaction vessel was removed from the liquid-nitrogen cold bath and quickly backfilled with 1 atm of CO_2, while the solution was still frozen. Upon thawing, the solution gradually turns purple and a colorless precipitate forms, and after 12 h, the solution has an intense purple color. The reaction was frozen again in liquid nitrogen, and the atmosphere changed to nitrogen. In the glovebox, the colorless precipitate was removed from the solution using a sintered-glass frit of medium porosity and washed with 3 × 10 mL of THF. The solvent of the purple filtrate was removed in vacuo. Both solids were analyzed using ^{1}H and ^{13}C NMR spectroscopy, identifying the purple reaction product as the known compound[25,27] $Cp_2Ta(H)(CO)$ (**5**) and the colorless solid as a mixture of [K([2.2.2]cryptand)]OH, [K([2.2.2]-cryptand)]$_2CO_3$, [K([2.2.2]cryptand)]HCO_3, and [K([2.2.2]-cryptand)]HCO_2.

5. ^{1}H NMR (C_6D_6, 300 MHz): δ 4.48 (d, *J* = 0.5 Hz, 10H, Cp*H*), −6.77 (s, 1H, Ta*H*). ^{13}C NMR (C_6D_6, 300 MHz): δ 165.2 (s, CO), 82.7 (s, Cp).

Colorless product. ^{1}H NMR (DMSO-d_6, 400 MHz): δ 8.58 (s, 0.05H, HCO_2^-), 3.56 (br s, 12H, *cryptand*), 3.52 (br s, 12H, *cryptand*), 2.51 (br s, 12H, *cryptand*). ^{13}C{^{1}H} NMR (DMSO-d_6, 101 MHz): δ 173.3 (s, HCO_2^-), 168.7 (s, CO_3^{2-}), 164.69 (s, HCO_3^-), 69.8 (s, *cryptand*), 67.0 (s, *cryptand*), 53.2 (s. *cryptand*).

Synthesis of $Cp_2Ta(\mu\text{-}H)_2Rh(dippp)$ (6). At ambient temperature in the glovebox, a solution of [RhCl(dippp)]$_2$ (119 mg, 0.14 mmol) in 10 mL of THF was added to a solution of **1** (214 mg, 0.29 mmol) in 20 mL of THF. The brown reaction mixture was stirred for 14 h and then evaporated to dryness. The crude product was extracted with 3 × 4 mL of benzene, the combined organic fractions were filtered through diatomaceous earth, and the solvent was removed in vacuo again. The remaining dark-red, sticky solid was extracted with *n*-pentane until the fractions became almost colorless, the combined pentane fractions were filtered through diatomaceous earth, and the solution was placed in the freezer. After 5 days, the light-red solution was removed with a syringe, and the dark-red crystals were washed with 4 × 1 mL of cold *n*-pentane and dried in vacuo to obtain complex **6** in 81 mg yield (0.11 mmol, 40%).

^{1}H NMR (C_6D_6, 400 MHz): δ 5.28 (s, 10H, *Cp*), 1.44 (m, 2H, dippp-CH_2), 1.23 (m, 4H, dippp-(CH_2)$_2$), 1.07 (dd, *J* = 14.4 and 7.1 Hz, 12H, CH(CH_3)$_2$), 0.88 (dd, *J* = 12.6 and 6.8 Hz, 12H, CH(CH_3)$_2$), 0.73 (m, 4H, C*H*(CH$_3$)$_2$), −15.26 (m, 2H, Ta(μ-*H*)$_2$Rh). ^{13}C{^{1}H} NMR (C_6D_6, 101 MHz): δ 85.5 (s, *Cp*), 27.2 (t, *J* = 11.8 Hz, dippp-(CH_2)$_2$), 23.7 (m, dippp-CH_2), 21.0 (t, *J* = 26.7 Hz, *C*H(CH$_3$)$_2$), 19.7 (s, CH(*C*H$_3$)$_2$), 18.5 (s, CH(*C*H$_3$)$_2$). ^{31}P{^{1}H} NMR (C_6D_6, 162 MHz): δ 39.8 (d, J_{RhP} = 143 Hz). UV−vis (298 K, THF): 227 (s), 305 (m), 368 (m), 500 (w) nm. Anal. Calcd for $C_{25}H_{46}P_2RhTa$: C, 43.36; H, 6.70. Found: C, 43.46; H, 6.76.

Reaction of 6 toward CO. ***Caution!*** *This reaction results in a pressure of greater than 1.5 atm within a sealed vessel upon warming to room temperature and was performed with great care and initially manipulated behind a blast shield.* At ambient temperature, compound **6** (15 mg, 22 μmol) was dissolved in 0.5 mL of C_6D_6, and the solution was placed in a flame-sealable NMR tube. The solution was degassed via three freeze−pump−thaw cycles and subsequently frozen in liquid nitrogen. The evacuated headspace was then backfilled with 0.9 atm of CO gas at liquid-nitrogen temperature. The NMR tube was flame-sealed with a torch, allowed to warm to ambient temperature behind a blast shield, and left untouched for 1 h; afterward, the reaction was monitored in regular intervals over 3 days using ^{1}H and ^{31}P NMR spectroscopy. After 3 days, the NMR spectra did not change, indicating the final formation of **5**[25,27] and **7**.

^{1}H NMR (C_6D_6, 300 MHz): δ 4.48 (d, *J* = 0.7 Hz, 10H, *Cp*), 1.58 (m, 4H, dippp), 1.42 (m, 2H, dippp), 1.04 (m, 12H, CH(CH_3)$_2$), 0.96 (m, 2H, dippp), 0.88 (m, 12H, ^{i}Pr(CH$_3$)$_2$), −6.77 (s, 1H, Ta*H*), −9.62

DOI: 10.1021/ic502976r
Inorg. Chem. 2015, 54, 2357−2366

(dt, J = 50.4 and 11.5 Hz, 1H, RhH). $^{13}C\{^1H\}$ NMR (C_6D_6, 151 MHz): δ 201.3 (dt, J = 68.7 and 9.1 Hz, RhCO), 82.7 (s, CpTa), 28.2 (t, J = 10.7 Hz, dippp-$(CH_2)_2$), 23.1 (t, J = 6.6 Hz, dippp-(CH_2)), 20.6 (t, J = 10.8 Hz, $CH(CH_3)_2$), 18.6 (t, J = 3.1 Hz, $CH(CH_3)_2$), 17.6 (s, $CH(CH_3)_2$). $^{31}P\{^1H\}$ NMR (C_6D_6, 121 MHz): δ 39.9 (d, J = 112.4 Hz).

Attempted Synthesis of $Cp_2Ta(\mu\text{-}H)_2Ru(H)(CO)(P^iPr_3)_2$ (8). In the glovebox, complex **1** (119 mg, 0.16 mmol) and $Ru(H)(Cl)(CO)(P^iPr_3)_2$ (79 mg, 0.16 mmol) were weighed into two separate Schlenk flasks and dissolved in 10 mL of THF each. The solution of **1** was cooled to 0 °C in an ice bath, and the solution of $Ru(H)(Cl)(CO)(P^iPr_3)_2$ was added dropwise via a cannula. During the addition, the reaction mixture turned dark brown. After the addition was complete, the reaction mixture was stirred for an additional 30 min at 0 °C and 30 min at ambient temperature. The solvent was removed in vacuo, and the crude product was extracted into 2 × 2 mL of toluene. The combined toluene fractions were concentrated to 0.3 mL in vacuo, 10 mL of pentane was added, and the solution was placed in a freezer at −35 °C for at least 1 h. The cold solution was filtered through diatomaceous earth, and the solvent was removed in vacuo to dryness to obtain compound **8** in 80% purity based on NMR techniques.

^1H NMR (C_6D_6, 400 MHz): δ 5.67 (s, 5H, Cp), 5.64 (s, 5H, Cp), 1.59 (m, 6H, $CH(CH_3)_2$), 1.01 (m, 36H, $CH(CH_3)_2$), −6.55 (tt, J = 25.4 and 4.6 Hz, 1H, term-RuH), −17.99 (m, 2H, Ta$(\mu\text{-}H)_2$Ru). $^{13}C\{^1H\}$ NMR (C_6D_6, 101 MHz): δ 85.1 (s, Cp), 27.6 (br s, $CH(CH_3)_2$), 20.2 (s, $CH(CH_3)_2$). The signal for the CO ligand could not be observed. $^{31}P\{^1H\}$ NMR (C_6D_6, 162 MHz): δ 70.0 (s, RuP^iPr_3).

Attempted Synthesis of $Cp_2Ta(\mu\text{-}H)_2Ru(H)(N_2)(P^iPr_3)_2$ (9). The synthesis was performed similarly to compound **8**, using **1** (50 mg, 69 μmol) and $Ru(H)(Cl)(N_2)(P^iPr_3)_2$ (34 mg, 70 μmol) as starting materials.

^1H NMR (C_6D_6, 400 MHz): δ 5.25 (s, 5H, Cp), 4.36 (s, 5H, Cp), 1.72 (m, 6H, $CH(CH_3)_2$), 1.12 (dd, J = 11.6 and 7.2 Hz, 6H, $CH(CH_3)_2$), −16.50 (m, 2H, Ta$(\mu\text{-}H)_2$Ru), −24.94 (m, 1H, term-RuH). $^{13}C\{^1H\}$ NMR (C_6D_6, 101 MHz): δ 88.3 (s, Cp), 87.4 (s, Cp), 28.8 (d, J = 16.1 Hz, $CH(CH_3)_2$), 20.67 (s, $CH(CH_3)_2$). $^{31}P\{^1H\}$ NMR (C_6D_6, 162 MHz): δ 71.3 (s, RuP^iPr_3).

■ ASSOCIATED CONTENT

Ⓢ Supporting Information

NMR spectral data, summarized X-ray crystallographic information, crystal structures, and crystallographic data in CIF format. This material is available free of charge via the Internet at http://pubs.acs.org.

■ AUTHOR INFORMATION

Corresponding Author

*E-mail: fryzuk@chem.ubc.ca.

Notes

The authors declare no competing financial interest.

■ ACKNOWLEDGMENTS

We thank NSERC of Canada for funding in the form of a Discovery Grant to M.D.F. and the German Academic Exchange Service (DAAD) for a postdoctoral fellowship to T.G.O.

■ DEDICATION

Dedicated to Professor Manfred Scheer on the occasion of his 60th birthday.

■ REFERENCES

(1) (a) Bullock, R. M.; Casey, C. P. *Acc. Chem. Res.* **1987**, *20*, 167−173. (b) Shibasaki, M.; Kanai, M.; Matsunaga, S.; Kumagai, N. *Acc. Chem. Res.* **2009**, *42*, 1117−1127.

(2) (a) Stephan, D. W. *Coord. Chem. Rev.* **1989**, *95*, 41−107. (b) Wheatley, N.; Kalck, P. *Chem. Rev.* **1999**, *99*, 3379−3419. (c) Cooper, B. G.; Napoline, J. W.; Thomas, C. M. *Catal. Rev.: Sci. Eng.* **2012**, *54*, 1−40.

(3) (a) Bau, R.; Teller, R. G.; Kirtley, S. W.; Koetzle, T. F. *Acc. Chem. Res.* **1979**, *12*, 176−183. (b) Venanzi, L. M. *Coord. Chem. Rev.* **1982**, *43*, 251−274.

(4) (a) Lewis, D. J.; Glover, P. B.; Solomons, M. C.; Pikramenou, Z. *J. Am. Chem. Soc.* **2011**, *133*, 1033−1043. (b) Fieser, M. E.; Mueller, T. J.; Bates, J. E.; Ziller, J. W.; Furche, F.; Evans, W. J. *Organometallics* **2014**, *33*, 3882−3890.

(5) Selected examples for heterobimetallic hydride complexes derived from adduct formation: (a) Leblanc, C.; Reynoud, J. F.; Moise, C. *J. Organomet. Chem.* **1983**, *244*, C24−C26. (b) Albinati, A.; Naegli, R.; Togni, A.; Venanzi, L. M. *J. Organomet. Chem.* **1987**, *330*, 85−100. (c) Casey, C. P.; Whiteker, G. T. *Inorg. Chem.* **1990**, *29*, 876−879. (d) Bakhmutov, V. I.; Visseaux, M.; Baudry, D.; Dormond, A.; Richard, P. *Inorg. Chem.* **1996**, *35*, 7316−7324. (e) Bakhmutov, V. I.; Vorontsov, E. V.; Boni, G.; Moise, C. *Inorg. Chem.* **1997**, *36*, 4055−4059. (f) Bakhmutov, V. I.; Vorontsov, E. V.; Bakhmutova, E. V.; Boni, G.; Moise, C. *Inorg. Chem.* **1999**, *38*, 1121−1125.

(6) Selected examples for heterobimetallic hydride complexes derived from protonolysis reactions: (a) Alvarez, D., Jr.; Caulton, K. G.; Evans, W. J.; Ziller, J. W. *Inorg. Chem.* **1992**, *31*, 5500−5508. (b) Ito, J.-I.; Shima, T.; Suzuki, H. *Organometallics* **2006**, *25*, 1333−1336. (c) Shima, T.; Hou, Z. *Organometallics* **2009**, *28*, 2244−2252. (d) O, W. W. N.; Kang, X.; Luo, Y.; Hou, Z. *Organometallics* **2014**, *33*, 1030−1043.

(7) Bruno, J. W.; Huffman, J. C.; Green, M. A.; Caulton, K. G. *J. Am. Chem. Soc.* **1984**, *106*, 8310−8312.

(8) (a) Alvarez, D., Jr.; Lundquist, E. G.; Ziller, J. W.; Evans, W. J.; Caulton, K. G. *J. Am. Chem. Soc.* **1989**, *111*, 8392−8398. (b) Lundquist, E. G.; Caulton, K. G.; Spencer, J. L. *Inorg. Synth.* **1990**, *27*, 26−30. (c) Poulton, J. T.; Folting, K.; Caulton, K. G. *Organometallics* **1992**, *11*, 1364−1372.

(9) (a) He, Z.; Neibecker, D.; Mathieu, R. *J. Organomet. Chem.* **1993**, *460*, 213−217. (b) He, Z.; Nefedov, S.; Lugan, N.; Neibecker, D.; Mathieu, R. *Organometallics* **1993**, *12*, 3837−3845. (c) Moldes, I.; Delavaux-Nicot, B.; Lugan, N.; Mathieu, R. *Inorg. Chem.* **1994**, *33*, 3510−3514. (d) Moldes, I.; Nefedov, S.; Lugan, N.; Mathieu, R. *J. Organomet. Chem.* **1995**, *490*, 11−19.

(10) (a) Shima, T.; Suzuki, H. *Organometallics* **2000**, *19*, 2420−2422. (b) Oishi, M.; Kato, T.; Nakagawa, M.; Suzuki, H. *Organometallics* **2008**, *27*, 6046−6049. (c) Oishi, M.; Suzuki, H. *Inorg. Chem.* **2009**, *48*, 2349−2351. (d) Oishi, M.; Kino, M.; Saso, M.; Oshima, M.; Suzuki, H. *Organometallics* **2012**, *31*, 4658−4661.

(11) (a) Baudry, D.; Ephritikhine, M. *J. Organomet. Chem.* **1986**, *311*, 189−192. (b) Freeman, J. W.; Arif, A. M.; Ernst, R. D. *Inorg. Chim. Acta* **1995**, *240*, 33−40. (c) Weng, W.-Q.; Arif, A. M.; Ernst, R. D. *J. Cluster Sci.* **1996**, *7*, 629−641. (d) Plois, M.; Hujo, W.; Grimme, S.; Schwickert, C.; Bill, E.; de Bruin, B.; Pöttgen, R.; Wolf, R. *Angew. Chem., Int. Ed.* **2013**, *52*, 1314−1318.

(12) Linn, D. E.; Halpern, J. *J. Am. Chem. Soc.* **1987**, *109*, 2969−2974.

(13) Selected examples for anionic oligohydride complexes synthesized by deprotonation of neutral hydride complexes: (a) Huffmann, J. C.; Green, M. A.; Kaiser, S. L.; Caulton, K. G. *J. Am. Chem. Soc.* **1985**, *107*, 5111−5115. (b) Bandy, J. A.; Berry, A.; Green, M. L. H.; Prout, K. *J. Chem. Soc., Chem. Commun.* **1985**, 1462−1464. (c) Hinman, J. G.; Abdur-Rashid, K.; Lough, A. J.; Morris, R. H. *Inorg. Chem.* **2001**, *40*, 2480−2481.

(14) Selected examples for anionic oligohydride complexes synthesized using hydride reagents: (a) Chan, A. S. C.; Shieh, H.-S. *J. Chem. Soc., Chem. Commun.* **1985**, 1379−1380. (b) Abdur-Rashid, K.; Gusev, D. G.; Landau, S. E.; Lough, A. J.; Morris, R. H. *J. Am. Chem. Soc.* **1998**, *120*, 11826−11827. (c) Gusev, D. G.; Lough, A. J.; Morris, R. H. *J. Am. Chem. Soc.* **1998**, *120*, 13138−13147. (d) Abdur-Rashid, K.; Gusev, D. G.; Lough, A. J.; Morris, R. H. *Organometallics* **2000**, *19*, 834−843.

DOI: 10.1021/ic502976r
Inorg. Chem. 2015, 54, 2357−2366

(15) Barron, A. R.; Hursthouse, M. B.; Motevalli, M.; Wilkinson, G. *J. Chem. Soc., Chem. Commun.* **1986**, 81−82.
(16) Morris, R. H. Non-classical hydrogen bonding along the pathway to the heterolytic splitting of dihydrogen. In *Recent Advances in Hydride Chemistry*; Peruzzini, M., Poli, R., Eds.; Elsevier Science: New York, 2002.
(17) (a) Francis, B. R.; Green, M. L. H.; Luong-thi, T.; Moser, G. A. *J. Chem. Soc., Dalton Trans.* **1976**, 1339−1345. (b) Lemenovski, D. A.; Nifant'ev, I. E.; Urazowski, I. F.; Perevalova, E. G.; Timofeeva, T. V.; Slovokhotov, Y. L.; Struchlov, Y. T. *J. Organomet. Chem.* **1988**, *342*, 31−44. (c) Green, M. L. H.; Hughes, A. K.; Mountford, P. *J. Chem. Soc., Dalton Trans.* **1991**, 1699−1704. (d) Fermin, M. C.; Stephan, D. W. *J. Am. Chem. Soc.* **1995**, *117*, 12645−12646. (e) Etkin, N.; Hoskin, A. J.; Stephan, D. W. *J. Am. Chem. Soc.* **1997**, *119*, 11420−11424. (f) Horáček, M.; Hiller, J.; Thewalt, U.; Polášek, M.; Mach, K. *Organometallics* **1997**, *16*, 4185−4191. (g) Hoskin, A. J.; Stephan, D. W. *Coord. Chem. Rev.* **2002**, *233*−*234*, 107−129. (h) Morse, P. M.; Shelby, Q. D.; Kim, D. Y.; Girolami, G. S. *Organometallics* **2008**, *27*, 984−993.
(18) (a) Lemenovskii, D. A.; Nifant'ev, I. E.; Zagorevskii, D. V. *Izv. Akad. Nauk SSSR, Ser. Khim.* **1985**, *8*, 1933. (b) Lemenovskii, D. A.; Nifant'ev, I. E.; Perevalova, E. G.; Tsiomo, S. N.; Efimov, N. K.; Zubanova, V. I. *Koord. Khim.* **1987**, *13*, 1623−1628. (c) Michaelidou, D. M.; Green, M. L. H.; Hughes, A. K.; Mountford, P.; Chernega, A. N. *Polyhedron* **1995**, *14*, 2663−2675.
(19) (a) Fryzuk, M. D.; Haddad, T. S.; Mylvaganam, M.; McConville, D. H.; Rettig, S. J. *J. Am. Chem. Soc.* **1993**, *115*, 2782−2792. (b) Fryzuk, M. D.; Love, J. B.; Rettig, S. J.; Young, V. G. *Science* **1997**, *275*, 1445−1447. (c) Fryzuk, M. D.; Johnson, S. A.; Rettig, S. J. *J. Am. Chem. Soc.* **1998**, *120*, 11024−11025. (d) Fryzuk, M. D. *Acc. Chem. Res.* **2009**, *42*, 127−133. (e) Ballmann, J.; Munhá, R. F.; Fryzuk, M. D. *Chem. Commun.* **2010**, *46*, 1013−1025. (f) Ballmann, J.; Yeo, A.; Patrick, B. O.; Fryzuk, M. D. *Angew. Chem., Int. Ed.* **2011**, *50*, 507−510.
(20) (a) Green, M. L. H.; Moreau, J. J. E. *J. Organomet. Chem.* **1978**, *161*, C25−C26. (b) Bunker, M. J.; De Cian, A.; Green, M. L. H.; Moreau, J. J. E.; Siganporia, N. *J. Chem. Soc., Dalton Trans.* **1980**, 2155−2161.
(21) Lantero, D. R.; Motry, D. H.; Ward, D. L.; Smith, M. R., III. *J. Am. Chem. Soc.* **1994**, *116*, 10811−10812.
(22) (a) Reynoud, J.-F.; Leboeuf, J.-F.; Leblanc, J.-C.; Moise, C. *Organometallics* **1986**, *5*, 1863−1866. (b) Sauvageot, P.; Sadorge, A.; Nuber, B.; Kubicki, M. M.; Leblanc, J.-C.; Moise, C. *Organometallics* **1999**, *18*, 2133−2138. (c) Sabo-Etienne, S.; Rodriguez, V.; Donnadieu, B.; Chaudret, B.; Abou el Makarim, H.; Barthelat, J.-C.; Ulrich, S.; Limbach, H.-H.; Moise, C. *New J. Chem.* **2001**, 55−62.
(23) Jonas, K.; Krüger, C. *Angew. Chem., Int. Ed. Engl.* **1980**, *19*, 520−537.
(24) Panda, T. K.; Gamer, M. T.; Roesky, P. W. *Organometallics* **2003**, *22*, 877−878.
(25) Persson, C.; Andersson, C. *Organometallics* **1993**, *12*, 2370−2371.
(26) (a) Barefield, E. K.; Parshal, G. W.; Tebbe, F. N. *J. Am. Chem. Soc.* **1970**, *92*, 5234−5235. (b) Foust, D. F.; Rogers, R. D.; Rausch, M. D.; Atwood, J. L. *J. Am. Chem. Soc.* **1982**, *104*, 5646−5650.
(27) Green, M. L. H.; Jousseaume, B. *J. Organomet. Chem.* **1980**, *193*, 339−344.
(28) Reynoud, J.-F.; Leblanc, J.-C.; Moise, C. *Organometallics* **1985**, *4*, 1059−1063.
(29) (a) Song, Y.; Jing, H.; Li, B.; Bai, D. *Chem.—Eur. J.* **2011**, *17*, 8731−8738. (b) *NMR Database, Spectrum-ID NC_24533*, Bio-Rad Laboratories, Inc.: Hercules, CA, 2014.
(30) (a) Ballmann, J.; Pick, F.; Castro, L.; Fryzuk, M. D.; Maron, L. *Inorg. Chem.* **2013**, *52*, 1685−1687. (b) Rankin, M. A.; Cummins, C. C. *J. Am. Chem. Soc.* **2010**, *132*, 10021−10023.
(31) (a) Brisdon, A. K. *Inorganic Spectroscopic Methods*; Oxford Science Publications: Oxford, U.K., 1998. (b) Solomon, E. I.; Lever, A. B. P. *Inorganic Electronic Structure and Spectroscopy*; John Wiley & Sons, Inc.: New York, 1999.
(32) Cordero, B.; Gómez, V.; Platero-Prats, A. E.; Revés, M.; Echeverria, J.; Cremades, E.; Barragán, F.; Alvarez, S. *Dalton Trans.* **2008**, 2832−2838.
(33) (a) Forniés-Camer, J.; Masdeu-Bultó, A. M.; Claver, C.; Tejel, C.; Ciriano, M. A.; Cardin, C. J. *Organometallics* **2002**, *21*, 2609−2618. (b) Cheliatsidou, P.; White, D. F. S.; de Bruin, B.; Reek, J. N. H.; Cole-Hamilton, D. J. *Organometallics* **2007**, *26*, 3265−3268.
(34) Findlay, A. E.; Leelasubcharoen, S.; Kuzmina, L. G.; Howard, J. A. K.; Nikonov, G. I. *Dalton Trans.* **2010**, *39*, 9264−9269.
(35) Fryzuk, M. D.; Piers, W. E.; Rettig, S. J.; Einstein, F. W. B.; Jones, T.; Albright, T. A. *J. Am. Chem. Soc.* **1989**, *111*, 5109−5121.
(36) Esteruelas, M. A.; Werner, H. *J. Organomet. Chem.* **1986**, *303*, 221−231.
(37) Coalter, J. N., III; Bollinger, J. C.; Huffman, J. C.; Werner-Zwanziger, U.; Caulton, K. G.; Davidson, E. R.; Gérard, H.; Clot, E.; Eisenstein, O. *New J. Chem.* **2000**, *24*, 9−26.

DOI: 10.1021/ic502976r
Inorg. Chem. 2015, 54, 2357−2366